journal

J. Am. Ceram. Soc., 79 [1] 239–47 (1996)

Structure Evolution in Hydrothermally Processed (<100°C) $BaTiO_3$ Films

Elliott B. Slamovich*,† and Ilhan A. Aksay*

Department of Chemical Engineering and Princeton Materials Institute, Princeton University, Princeton, New Jersey 08544-5263

Thin films of cubic $BaTiO_3$ were processed hydrothermally at 40°–80°C by reacting thin layers of titanium organometallic liquid precursors in aqueous solutions of either $Ba(OH)_2$ or a mixture of NaOH and $BaCl_2$. All films (thickness ~1 μm) were polycrystalline with grain sizes ranging from nano- to micrometer dimensions. $BaTiO_3$ formation was facilitated by increasing $[OH^-]$, $[Ba^{2+}]$, and the temperature. The film structure was related to the nucleation and growth behavior of the $BaTiO_3$ particles. Films processed at relatively low $[OH^-]$, $[Ba^{2+}]$, and temperatures were coarse grain and opaque, but increasing $[OH^-]$, $[Ba^{2+}]$, and temperature caused the grain size to decrease, resulting in transparent films.

I. Introduction

THE tetragonal polymorph of $BaTiO_3$ is a well-known ferroelectric material used in a broad variety of device applications. The cubic form of $BaTiO_3$, while not ferroelectric, has a high dielectric constant suitable for capacitors in electronic circuits.[1] Sol–gel processing allows one to fabricate $BaTiO_3$ and related materials with a high degree of chemical homogeneity and at relatively low temperatures compared with traditional methods.[2] However, heat treatments in excess of 700°C are required to remove residual organics and form the desired crystalline phase.[3] This requirement makes the coprocessing of ceramics with semiconductors difficult, and the formation of polymer/ceramic composites impossible.

Hydrothermal processing is a route to process crystalline ceramics below 100°C. It involves the formation of crystalline materials from reactants in an aqueous medium under strongly alkaline conditions. Hydrothermal processing is used to fabricate large single crystals of quartz via seeding, and in the formation of zeolites from aluminosilicate gels.[4] In 1988, Lilley and Wusirika processed monosized powders of $BaTiO_3$ by dispersing TiO_2 powders in a concentrated solution of $Ba(OH)_2$.[5] Dogan *et al.* used transmission electron microscopy (TEM) to observe the formation of hydrothermally derived $BaTiO_3$ powders in a solution of $Ba(OH)_2$ with TiO_2 particles.[6] Their observations showed that the TiO_2 initially dissolved in the aqueous $Ba(OH)_2$ and led to the nucleation of nanometer-sized $BaTiO_3$ particles in cubic phase.

Calculations defining the thermodynamics of hydrothermal processing were performed by Lencka and Riman, who derived stability diagrams outlining the requirements to synthesize $BaTiO_3$ among other materials.[7] Their results showed that successful processing of $BaTiO_3$ required a pH > 12, and a barium concentration on the order of 10^{-4} molal or higher. The modeling also showed that it is possible to process $BaTiO_3$ at room temperature, although this has yet to be done experimentally. Finally, they demonstrated the importance of eliminating CO_2 from the reaction vessel to avoid the formation of $BaCO_3$.

Yoshimura and co-workers were the first to demonstrate the utility of hydrothermal processing to form thin films by fabricating a variety of perovskite materials.[8] They produced films of $BaTiO_3$ by depositing sputtered titanium metal films onto polymer or glass substrates, followed by a combined hydrothermal/electrochemical treatment at temperatures in excess of 100°C using an autoclave. Bendale *et al.* used a hydrothermal/electrochemical approach to grow films of $BaTiO_3$ on titanium metal substrates at temperatures as low as 55°C.[9] Their study indicated that a layer of titanium oxide acted as a precursor for the formation of $BaTiO_3$. Consistent with hydrothermal processing of powders, $BaTiO_3$ film formation was favored in highly alkaline CO_2-free environments.

The methods for $BaTiO_3$ film processing described above use sputtering techniques to process thin titanium precursor layers, or rely on electrochemical reactions or elevated temperature/pressure environments to promote film formation. The approach described in this paper uses hydrothermal processing to form films of $BaTiO_3$ from organometallic liquid precursors. $BaTiO_3$ film thickness is determined by the thickness of the precursor layer, which is controlled by the rheology of the liquid precursor, and is limited to thicknesses of ~1 μm, above which crack-free films could not be processed.[2] The precursors are reacted to form $BaTiO_3$ without an applied electric field and are processed at 80°C (or below) and atmospheric pressure. We also investigate the relationship between film structure and hydrothermal processing conditions, showing that small variations in temperature, pH, and barium concentration lead to dramatic changes in the nucleation behavior of the $BaTiO_3$ particles, which in turn affect film structure.

II. Experimental Procedure

Hydrothermally derived films of $BaTiO_3$ were processed by reacting films of titanium organometallic liquid precursors in aqueous solutions containing barium at a pH >12. Films of titanium diisopropoxide bis(ethylacetoacetate) (TIBE) (Gelest Chemical, Tullytown, PA) were processed by spin coating a thin layer (<1 μm) of the precursor (diluted 1:1 by volume with 2-propanol) onto a polystyrene substrate (0.2 mm thickness, 10 mm × 10 mm). To facilitate handling, the substrate was attached with double-sided tape to a 10 mm ×15 mm × 2 mm slide of PMMA. The PMMA slide was in turn attached to a spin coater, and enough precursor was applied with a pipette to cover the substrate. The spin coater was run at 10 kRPM for 5 s. Spin coating was repeated with a second coating of the precursor to get thicker films. The films were dried in a desiccator into which a small beaker of 2-propanol was placed to slow evaporation. Despite this, the films invariably cracked during drying. Small additions of Kraton D1102 (Shell Chemical, Belpre, OH), a block copolymer of polystyrene, and polybutadiene (70% polybutadiene by weight) were used to maintain the

W. A. Schulze—contributing editor

Manuscript No. 193311. Received August 16, 1994; approved August 17, 1995.
Supported by a URI program through the U.S. Army Research Office (Grant No. DAAL03-92-G-0241), with partial support through a NEDO program.
*Member, American Ceramic Society.
†Present address: School of Materials Engineering, Purdue University, West Lafayette, IN 47907.

mechanical integrity of the low-molecular-weight precursor films during drying.[10] Then the polymer (relative to TIBE) was dissolved into a solution of TIBE and toluene (1:1 by volume) and coated onto glass substrates (toluene etches polystyrene) as described above.

$Ba(OH)_2$ solutions were made from H_2O that had been boiled for 15 min to remove dissolved CO_2. After dissolution of $Ba(OH)_2$ in warm H_2O (>50°C), the solution was filtered, to remove any $BaCO_3$ formed on the solution surface, into a polyethylene bottle. The bottle was flushed with nitrogen, sealed, and kept in an oven at 40°C or higher (depending on the concentration of $Ba(OH)_2$) to avoid precipitation of $Ba(OH)_2$. To vary the alkalinity and barium concentration independently, solutions were fabricated in a similar manner from a combination of NaOH and $BaCl_2$. The pH of the $Ba(OH)_2$ and NaOH/$BaCl_2$ solutions was measured as a function of concentration and temperature using an ion analyzer (Model 901, Orion Research, Boston, MA) and a Ross combination pH electrode. pH measurements were performed in a controlled temperature water bath; the analyzer was recalibrated at each temperature, because the pH of the buffer solution was temperature dependent.

$BaTiO_3$ films were fabricated by placing the coated substrates into bottles containing solutions of $Ba(OH)_2$ or NaOH/$BaCl_2$, purging with nitrogen, and placing the bottle in an oven. The substrates were held on the bottom of the bottle using a piece of Teflon for ballast. The concentration of $Ba(OH)_2$ was varied between 0.20 and 2.0*M*, and the films were processed at 40°–80°C, for 4–72 h. For NaOH/$BaCl_2$ solutions, the NaOH and $BaCl_2$ concentrations were varied from 0.50 to 5.0*M* and 0.1 to 1.0*M*, respectively. After the hydrothermal treatment, the films were rinsed in warm CO_2-free water to remove any residual $Ba(OH)_2$ from the film surface. To examine the initial stages of film growth, precursor films coated onto polystyrene substrates were exposed to 0.50 and 1.0*M* solutions of $Ba(OH)_2$ at 70°C for times ranging from 15 s to 10 min. The hydrothermal reaction was quenched by rinsing the film in warm H_2O to remove $Ba(OH)_2$, followed by a second rinse in cold H_2O.

The films were characterized by X-ray diffraction (XRD) (XRD 3720, Philips, Mahwah, NJ) using Cu$K\alpha$ radiation and a scan rate of 0.75°/min from 15° to 65° 2θ, and their structure was examined in a scanning electron microscope (SEM) (SEM 515, Philips) by mounting the films on aluminum stubs with carbon paint and coating the film surface with gold. The films were also characterized by Fourier transform infrared spectroscopy (FTIR) (IR/44, IBM Instruments, (through Nicolet Instruments, Madison, WI)), and their chemical composition was analyzed by wavelength-dispersive X-ray spectroscopy (WDS) with an electron beam microprobe (SX-50, Cameca Instruments, Stamford, CT). To obtain FTIR spectra in transmission, the undiluted TIBE precursor was applied via spin coating across the surface of a 200 mesh gold microscopy grid, the liquid precursor filling the hexagonal holes of the grid. The coated grids were given the same hydrothermal treatment as the films processed on substrates. The grids were aligned in the IR beam, and a background spectrum was taken using an uncoated grid. A typical spectrum consisted of 600 scans performed with 2 cm^{-1} resolution. Coated grids also were used for quantitative analysis of the films in the electron beam microprobe, thereby avoiding complications arising from the interaction of the electron beam with the substrate. Peak overlap of the titanium $K\alpha$ and barium $L\alpha$ lines complicated quantitative measurement of barium and titanium by energy-dispersive spectroscopy (EDS). However, barium and titanium may be resolved by using a lithium fluoride monochromator via WDS. WDS was also used to measure the concentration of oxygen, sodium, and silicon (impurities that were present above background level according to EDS). Analysis was typically performed at 15 kV accelerating voltage with a beam current of 20 nA and a 1 μm probe diameter.

III. Results and Observations

The pH of the $Ba(OH)_2$ solutions increased with concentration but decreased with increasing temperature (Fig. 1(a)). The pH of alkaline solutions typically decreases with temperature due to the temperature dependence of the dissociation constant of water.[11] The experimental curves were parallel to the pH calculated from Debye–Hückel theory.[11] The NaOH/$BaCl_2$ solutions had the same temperature dependence (Fig. 1(b)), with additions of $BaCl_2$ resulting in a decrease in the solution pH. Additions of neutral salts in excess of 0.5 molal lower solution pH.[11]

The ability to form hydrothermal $BaTiO_3$ films depended strongly on the processing conditions of temperature, $Ba(OH)_2$ concentration (or NaOH/$BaCl_2$ concentration), and time. All films discussed below were processed for 4 h. As shown in Table I, $BaTiO_3$ formed more readily with increasing temperature and $Ba(OH)_2$ concentration. For 0.20*M* $Ba(OH)_2$ solutions, no film formation was observed, even up to the highest processing temperature of 80°C. In 0.50*M* $Ba(OH)_2$ solutions, $BaTiO_3$ formed at 60°C and above. For $Ba(OH)_2$ concentrations 0.75*M* and above, $Ba(OH)_2$ precipitated from solution before the lower temperature limit of film formation was reached. NaOH and $BaCl_2$ have a higher solubility in H_2O at low temperatures compared to $Ba(OH)_2$. Therefore, $BaTiO_3$ films were processed in NaOH/$BaCl_2$ solutions at temperatures as low as

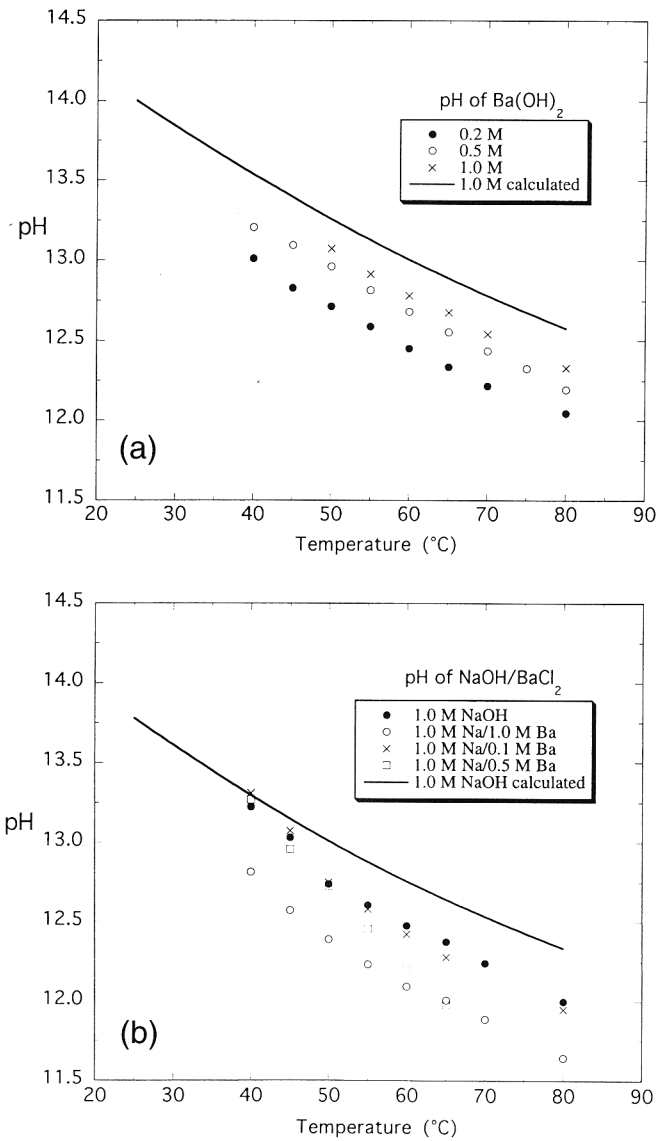

Fig. 1. (A) pH of aqueous $Ba(OH)_2$ solutions as a function of temperature. Solid line is pH for 1.0*M* $Ba(OH)_2$ calculated from Debye–Hückel theory. (B) pH of aqueous NaOH/$BaCl_2$ solutions as a function of temperature. Solid line is pH for 1.0*M* NaOH calculated from Debye–Hückel theory.

Table I. Formation of $BaTiO_3$ after 4 h Hydrothermal Treatment†

$[Ba(OH)_2]$	80°C	60°C	50°C	40°C
0.2*M*	X	X	X	X
0.5*M*	+	+	X‡	X
0.75*M*	+	+	+	ppt.
1.0*M*	+	+	+	ppt.
2.0*M*	+	+	ppt.	ppt.

†X = no $BaTiO_3$ observed; + = $BaTiO_3$ observed; ppt. = precipitation of $Ba(OH)_2$.
‡$BaTiO_3$ observed after 24 h.

Table II. Formation of $BaTiO_3$ after 4 h and 72 h Hydrothermal Treatment†

$[NaOH]/[BaCl_2]$	80°C	60°C	40°C	40°C/72 h
0.5*M*/1.0*M*	+	X	X	X
1.0*M*/0.1*M*	+	X	X	X
1.0*M*/0.5*M*	+	+	X	X
1.0*M*/1.0*M*	+	+	X	X
2.0*M*/1.0*M*	+	+	X	+
5.0*M*/1.0*M*	+	+	+‡	+‡

†X = no $BaTiO_3$ observed; + = $BaTiO_3$ observed. ‡Limited precipitation of $NaOH/BaCl_2$.

40°C. Table II shows that $BaTiO_3$ formation was facilitated by increasing both NaOH and $BaCl_2$ concentration and by raising the temperature.

The hydrothermally derived films exhibited colorful interference patterns in reflected light, much like soap bubbles and oil films. Depending on the processing conditions, the films ranged from transparent to optically opaque, the higher temperatures and $Ba(OH)_2$ (or $NaOH/BaCl_2$) concentrations producing transparent films.

(1) Structural and Chemical Characterization

XRD on selected films (Fig. 2) confirmed that they were composed of polycrystalline $BaTiO_3$. Peak broadening, suggesting that films were composed of submicrometer grains, obfuscated the distinction between cubic and tetragonal $BaTiO_3$. However, stabilization of the high-temperature phase has been observed in fine grain titanates and is attributed to a particle size effect.[12,13]

FTIR spectra are shown in Fig. 3. The unreacted TIBE precursor displayed a spectrum similar to that for titanium isopropoxide acetylacetonate (Ti(acac)) (Fig. 3(a)).[14] The absorption band at approximately 1700 cm^{-1} indicated the presence of free ethylacetylacetone.[14] However, the presence of Ti–O and C–O absorption bands at 620 and 1000 cm^{-1}, respectively, suggested that the precursor was relatively stable with respect to hydrolysis by water vapor in the laboratory. Exposure to 1.0*M* $Ba(OH)_2$ for 1 min at 70°C showed that the precursor hydrolyzed rapidly coincident with the formation of $BaTiO_3$ (450–825 cm^{-1}) (Fig. 3(b)). At this pH, TiO_2 solubility is high, and consequently no evidence for the condensation of TiO_2 was observed. Bands at 856, 1057, and 1400–1500 cm^{-1} correspond to $BaCO_3$ formed on the film surface during processing or transferred to the film surface as the grid was removed from the $Ba(OH)_2$ reaction solution (invariably a fine layer of $BaCO_3$ formed on the surface of the $Ba(OH)_2$ solutions). The broad band at 2800–3600 cm^{-1} arose from the antisymmetric and symmetric stretchings of bound H_2O and OH groups, while a more narrow band centered at 1572 cm^{-1} corresponded to HOH bending.[15] Bound hydroxyls are invariably found in hydrothermally derived materials and are most commonly removed by heating.[16] Further treatment in $Ba(OH)_2$ caused the growth of the $BaTiO_3$ band (Fig. 3(c)), and scattering of the IR beam by the $BaTiO_3$ particles resulted in the formation of a broad absorption starting at 2000 cm^{-1}. The superposition of the broad absorption and the H_2O/OH band produced the sharp transition peaking at 3510 cm^{-1}. In the hydrothermal reaction, $Ba(OH)_2$ served both to hydrolyze the TIBE precursor and to promote the formation of $BaTiO_3$. Alternatively, the same result is expected if the precursor is first hydrolyzed (i.e., with H_2O) and then reacted with $Ba(OH)_2$ (or $NaOH/BaCl_2$).

Microprobe analysis of the $BaTiO_3$ films is summarized in Tables III and IV. The data for $BaTiO_3$ films processed in 1.0*M* $Ba(OH)_2$ at 70°C were averaged from 30 data points taken from three different films, while the data for 1.0*M* NaOH/1.0*M* $BaCl_2$ were averaged from 10 points in one film. There are a number of possible reasons why the weight percent analysis in Table III does not total 100%. Penetration of the electron beam through the entire thickness of the thin film and porosity in the

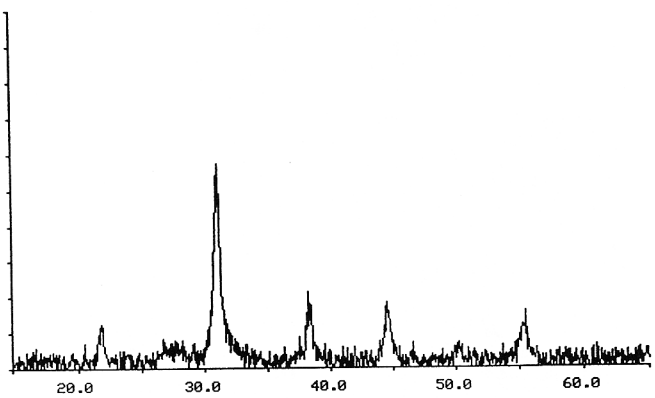

Fig. 2. Typical XRD pattern of a hydrothermally processed $BaTiO_3$ film. This particular film was processed in 1.0*M* $Ba(OH)_2$ at 70°C for 4 h.

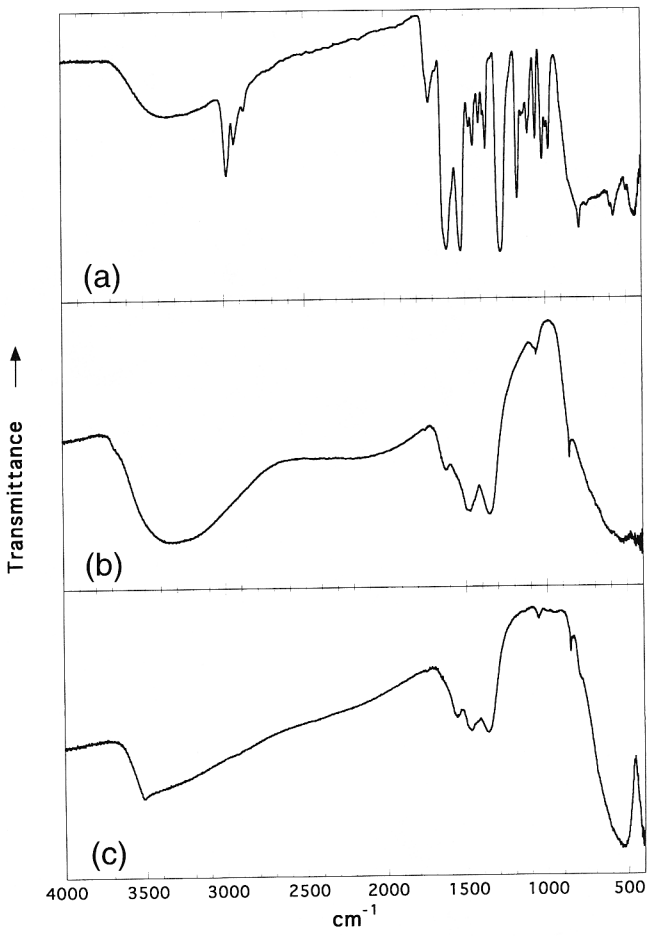

Fig. 3. FTIR spectra of (A) TIBE precursor, (B) TIBE precursor after 1 min in 1.0*M* $Ba(OH)_2$ at 70°C, (C) after 2 h in 1.0*M* $Ba(OH)_2$ at 70°C showing fully developed absorption band for $BaTiO_3$.

Table III. Composition of $BaTiO_3$ Films Processed for 4 h in 1.0*M* $Ba(OH)_2$ at 70°C

Element	wt%	at.%	SD
Ba	55.30	18.47	1.03
Ti	18.04	17.28	0.82
O	21.88	63.02	1.37
Si	0.58	0.96	0.38
Na	0.08	0.16	0.02
Total	95.88	100	30 pts analyzed

Table IV. Composition of $BaTiO_3$ Films Processed for 4 h in 1.0*M* NaOH/1.0*M* $BaCl_2$ at 70°C

Element	wt%	at.%	SD
Ba	55.90	18.58	1.94
Ti	19.80	18.87	0.98
O	21.40	60.93	0.77
Si	0.24	0.40	0.03
Na	0.36	0.72	0.37
Total	97.70	100	10 pts analyzed

film will result in errors, because the calibration standards for quantitative analysis are generally fully dense bulk materials. Also, the presence of impurities that were not analyzed (i.e., carbon) leads to weight percent totals below 100%. The purity of the $BaTiO_3$ films depended on the purity of the hydrothermal solution, since the films tended to incorporate dissolved impurities. $BaCO_3$ formed readily from any CO_2 dissolved in solution. Even though care was taken to minimize the exposure of the solution to CO_2, a CO_2-free environment is needed to completely eliminate contamination.[17] In addition, $BaCO_3$ is a common impurity in $Ba(OH)_2$, which may explain why the Ba-to-Ti ratio was greater than unity for $BaTiO_3$ films fabricated in $Ba(OH)_2$ solutions. Na and Si were common impurities, with Si more prevalent in films fabricated in $Ba(OH)_2$, and Na coming from NaOH/$BaCl_2$ solutions. Sodium can be avoided by using organic bases (i.e., $(CH_3)_4NOH$) in the place of NaOH. Silica contamination most likely came from the glassware used to prepare the hydrothermal solutions. Excess oxygen (O/Ba > 3) arose from Na and Si impurities, and, as indicated by FTIR, the presence of bound H_2O and OH groups.

(2) Film Morphology

Examination of the films by SEM showed the effects of $Ba(OH)_2$ concentration (Fig. 4) and temperature (Fig. 5) on the $BaTiO_3$ film structure. Increasing the $Ba(OH)_2$ concentration caused the average grain size to decrease from 0.25 μm for 0.50*M* $Ba(OH)_2$ to 0.05 μm for 2.0*M* $Ba(OH)_2$. Increasing the temperature had a similar effect. $BaTiO_3$ films processed in 1.0*M* $Ba(OH)_2$ at 50°C had a coarse texture due to a large average grain size of approximately 0.50 μm, while films processed in the same solution at 80°C had a smaller average grain size and a much smoother texture. The effects of temperature and $Ba(OH)_2$ concentration on the grain size of hydrothermally derived $BaTiO_3$ films are summarized in Fig. 6. The structural observations explain why fine grain films were transparent and coarse grain films opaque. A grain size approaching the film thickness led to the development of discontinuities or large pores in the film that scatter light. This phenomenon has been observed in thin films of metals and ceramics.[18–20] The fine grain films were transparent, because any porosity present was

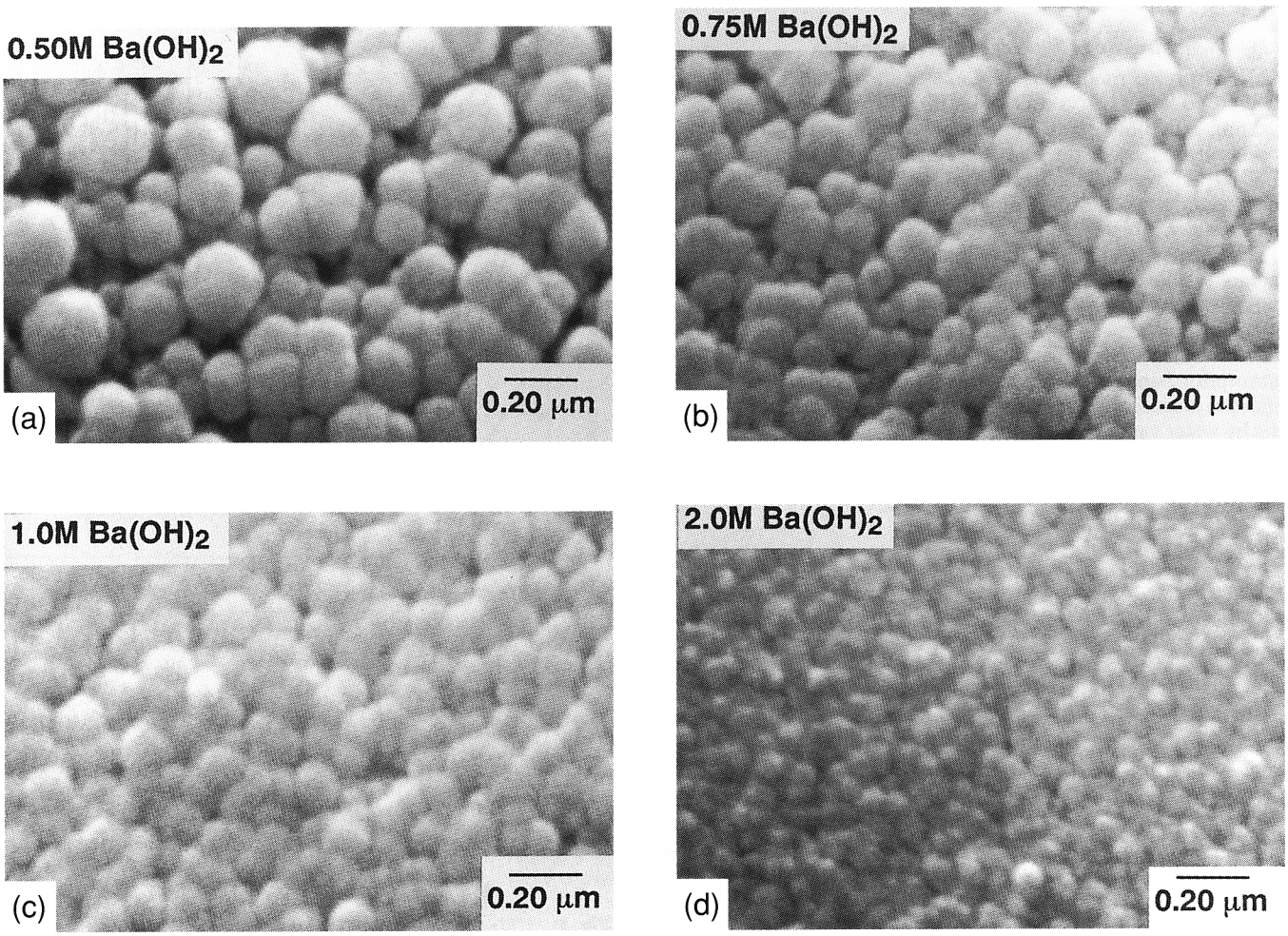

Fig. 4. Microstructure of $BaTiO_3$ films processed at 80°C for 4 h in (A) 0.5*M* $Ba(OH)_2$, (B) 0.75*M* $Ba(OH)_2$, (C) 1.0*M* $Ba(OH)_2$, (D) 2.0*M* $Ba(OH)_2$.

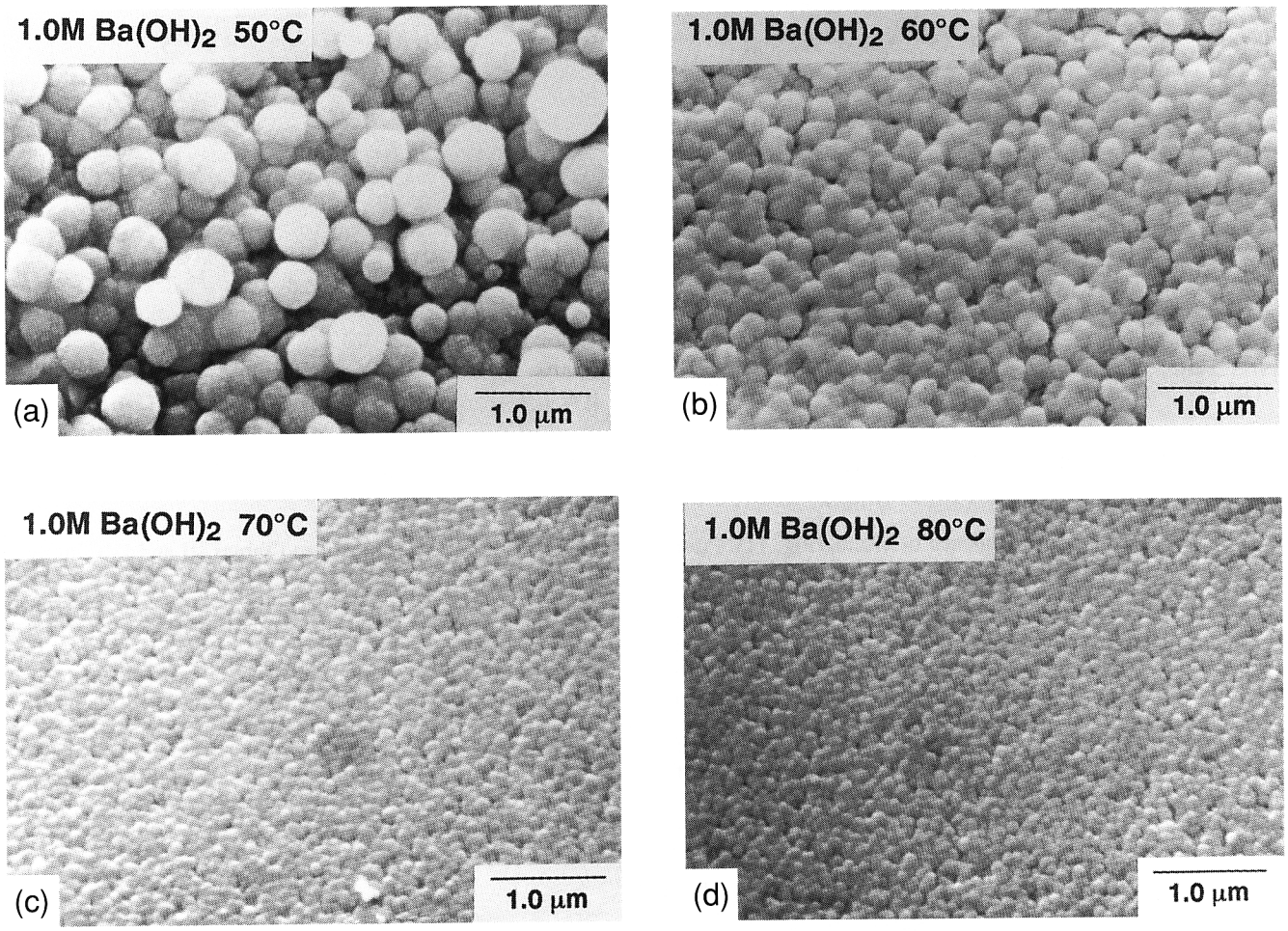

Fig. 5. Microstructure of $BaTiO_3$ films processed in 1.0*M* $Ba(OH)_2$ for 4 h at (A) 50°C, (B) 60°C, (C) 70°C, (D) 80°C.

too small to scatter light. Similar trends were observed for films fabricated from aqueous solutions of NaOH and $BaCl_2$. Figures 7 and 8 show the effects of varying NaOH and $BaCl_2$ concentration independently. Increasing $[OH^-]$ and $[Ba^{2+}]$ at constant temperature resulted in a much finer grain film. The films shown in Figs. 7(a) and 8(b) were made from solutions of the same composition at 60° and 80°C, respectively. As in the 1.0*M* $Ba(OH)_2$ solutions, the grain size decreased dramatically with increasing temperature.

Figures 9 and 10 show the early stages of film growth, captured by quenching the hydrothermal reaction after short reaction times, for films fabricated in 1.0*M* and 0.5*M* $Ba(OH)_2$ solutions at 70°C. After 1 min in 1.0*M* $Ba(OH)_2$, the $BaTiO_3$ particles completely covered the precursor film surface (Fig. 9(c)), while relatively few particles formed upon exposure to 0.5*M* $Ba(OH)_2$ over the same time period (Fig. 10(a)). However, the growth rate of the particles on each film was similar, the particles formed in 0.5*M* $Ba(OH)_2$ being approximately the same size or larger than those formed in 1.0*M* $Ba(OH)_2$. These observations indicate that the difference in film texture was due to the greater nucleation rate of $BaTiO_3$ particles on the precursor film exposed to 1.0*M* $Ba(OH)_2$. During film growth, $BaTiO_3$ particles established a two-dimensional percolating network and subsequently impinged upon one another, inhibiting further growth. Particles formed in 0.5*M* $Ba(OH)_2$ grew to a larger size before impinging upon one another by virtue of their slower nucleation rate. In contrast, the rapid nucleation rate of the film processed in 1.0*M* $Ba(OH)_2$ resulted in the formation of a percolating network at a much finer particle size, thereby decreasing the average particle size of the film.

IV. Discussion

A detailed mechanism of the hydrothermal formation of $BaTiO_3$ is its own topic.[21] However, based on the information available in the sol–gel literature, the hydrothermal formation of $BaTiO_3$ from films of organometallic precursors can be

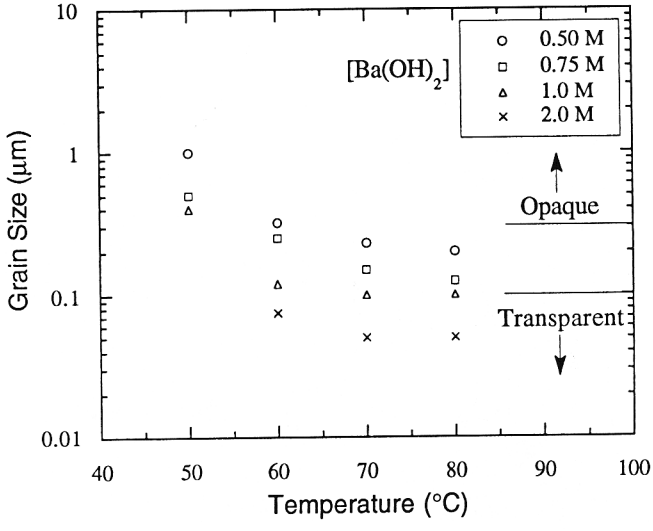

Fig. 6. Grain size of $BaTiO_3$ films as a function of temperature and $Ba(OH)_2$ concentration.

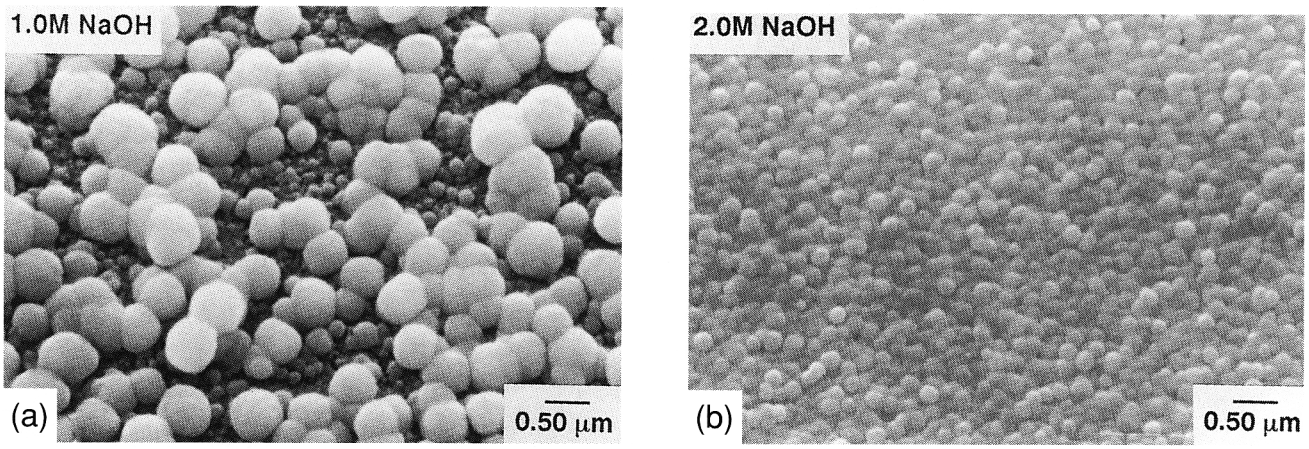

Fig. 7. Microstructure of $BaTiO_3$ films processed at 60°C for 4 h in (A) 1.0*M* NaOH/1.0*M* $BaCl_2$, (B) 2.0*M* NaOH/1.0*M* $BaCl_2$.

described by the following sequence of events (Fig. 11). Prior to hydrothermal treatment, the partially hydrolyzed TIBE precursor forms a viscous film on the surface of the substrate. Unless polymers are added, the volume change associated with solvent evaporation causes the film to crack. Upon exposure to aqueous $Ba(OH)_2$, the hydrolysis of TIBE may be analogous to that of titanium isopropoxide, resulting in a network of titanium hydroxides or oxohydroxides.[2] The aqueous hydrothermal solution permeates the film, causing the nucleation and growth of $BaTiO_3$ particles. This process can be rapid, with evidence of formation after only 15 s in 1.0*M* $Ba(OH)_2$ at 70°C (Fig. 9(a)). While $BaTiO_3$ appears to nucleate first on the film surface, titanium is not present in excess (Tables III and IV), implying that barium infiltrates throughout the depth of the precursor film to form $BaTiO_3$. The apparent ability of barium to permeate the surface layer of $BaTiO_3$ calls into question the utility of hydrothermal processing to process dense, pinhole-free films. Measurements of dielectric properties as well as further structural characterization will be required to address this concern.

The ability to form films of $BaTiO_3$ followed trends similar to those predicted by Lencka and Riman,[7] wherein the calculated stability of $BaTiO_3$ under hydrothermal conditions increases with pH and with barium concentration. Increasing the pH (by increasing the $[OH^-]$) and increasing the Ba concentration

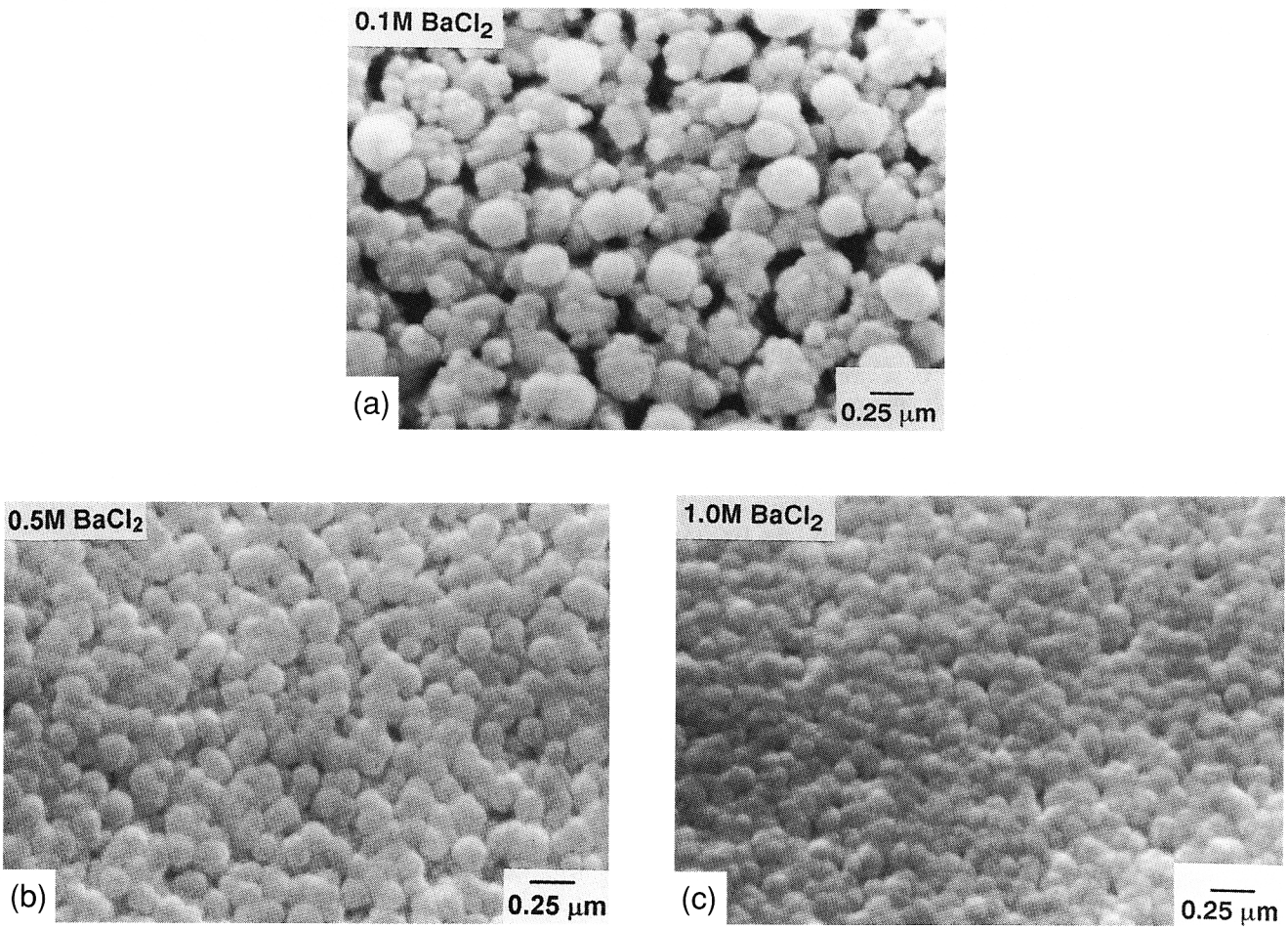

Fig. 8. Microstructure of $BaTiO_3$ films processed at 80°C for 4 h in (A) 1.0*M* NaOH/0.1*M* $BaCl_2$, (B) 1.0*M* NaOH/0.5*M* $BaCl_2$, (C) 1.0*M* NaOH/1.0*M* $BaCl_2$.

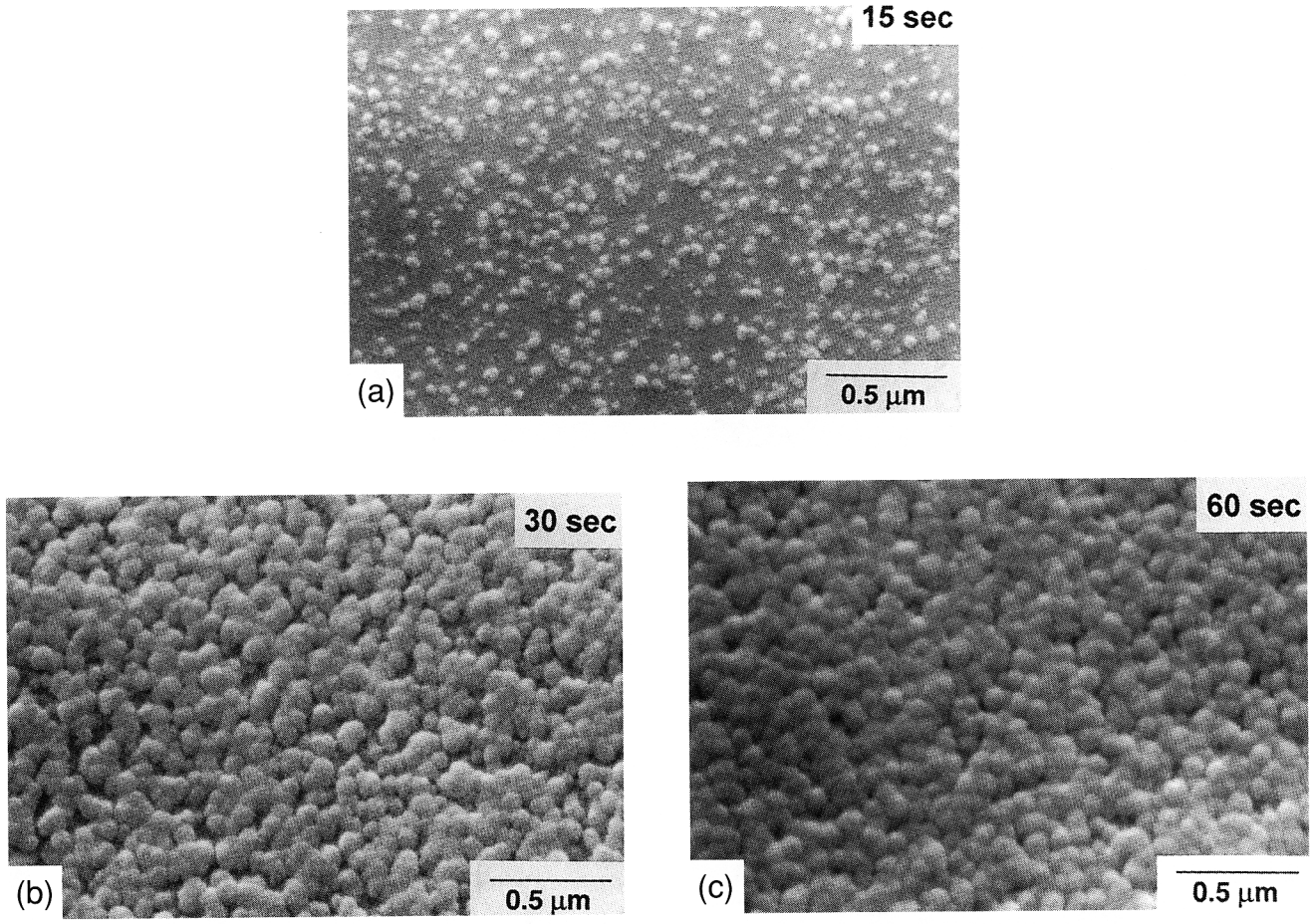

Fig. 9. Growth of a $BaTiO_3$ film in 1.0*M* $Ba(OH)_2$ at 70°C after (A) 15 s, (B) 30 s, (C) 1 min.

moved the system further into the region of stability toward $BaTiO_3$ formation. The effect of temperature is not as easy to interpret because, as shown by the pH measurements, pH and temperature are not independent variables. The stability boundary for $BaTiO_3$ moves to lower pH with increasing temperature.[7] However, the temperature dependence on pH of the stability boundary and the hydrothermal solution is approximately equal. Therefore, changing the temperature should result in no net change in the relative position of the solution pH with respect to the stability boundary. However, regarding the kinetics for mass transport, temperature will have a strong effect on the ability of ions to migrate through the hydrolyzed TIBE precursor layer. Increasing the temperature should enhance the diffusivity of ionic species, thereby facilitating the nucleation and growth of $BaTiO_3$.

Films processed in 0.2*M* $Ba(OH)_2$ failed to produce $BaTiO_3$ after 4 h, despite lying in a region of stability for $BaTiO_3$ formation. This result does not preclude the formation of $BaTiO_3$ with longer exposure times. Occurrence of an induction or incubation period before crystallization is commonly observed during the hydrothermal synthesis of zeolites, and the amount of time before the first observation of crystallites decreases with increasing temperature and pH.[4] This phenomenon was displayed by the hydrothermally derived $BaTiO_3$ films. Exposure to 0.5*M* $Ba(OH)_2$ at 50°C for 24 h, and 2.0*M* NaOH/1.0*M* $BaCl_2$ at 40°C for 72 h, produced films of submicrometer $BaTiO_3$ particles, whereas no films were observed after 4 h.

To supplement our observations, other examples may be found in the literature regarding the effects of processing conditions on the morphology of hydrothermally derived $BaTiO_3$ films and powders. Dutta and Gregg fabricated both micrometer-sized tetragonal and submicrometer-sized cubic powders by treating TiO_2 in the presence of NaOH and either $BaCl_2$ (producing the larger tetragonal particles) or $Ba(OH)_2$.[17] In both cases the samples were heated to 240°C for 7 days. The formation of the larger particles was attributed to the presence of Cl^-. However, it is consistent with our observations that substitution of $BaCl_2$ for $Ba(OH)_2$ should lower the $[OH^-]$, leading to a slower nucleation rate and thereby larger particles. Hertl[22] processed $BaTiO_3$ powders by mixing crystalline TiO_2 nanoparticles with aqueous $Ba(OH)_2$. He observed that the surface area of the $BaTiO_3$ powders increased with increasing $Ba(OH)_2$ concentration, implying that the average particle size decreased as observed above. He used a model combining diffusional and topochemical growth of $BaTiO_3$ on TiO_2 particles to explain the reaction kinetics. However, his model is not suitable to explain the variation in $BaTiO_3$ particle size with processing conditions, because the $BaTiO_3$ particle size should be fixed by the size of TiO_2 particles. The ability to nucleate particles directly from the amorphous precursor suggests that a dissolution/precipitation mechanism similar to that described by Dogan *et al.*[6] may be operative during $BaTiO_3$ film formation. Bendale *et al.*, fabricating $BaTiO_3$ on Ti metal substrates by an electrochemical/hydrothermal method, observed an increase in grain size with decreasing temperature.[9] They postulated that the large grains formed at heterogeneities created by the dielectric breakdown of the film; however, our observations indicated that decreasing the temperature decreased the particle nucleation rate, which is a more plausible explanation for the increase in grain size.

The structural evolution of the films (Figs. 9 and 10) was consistent with Avrami type nucleation and growth; i.e., particles continuously nucleated throughout the transformation, and termination occurred by the impingement of adjacent particles growing at a constant rate.[23,24] Therefore, a decrease in particle size stemmed from an increase in the nucleation rate relative to the growth rate. Arguments similar to those used for film formation apply to the nucleation behavior. Increasing $[OH^-]$ and

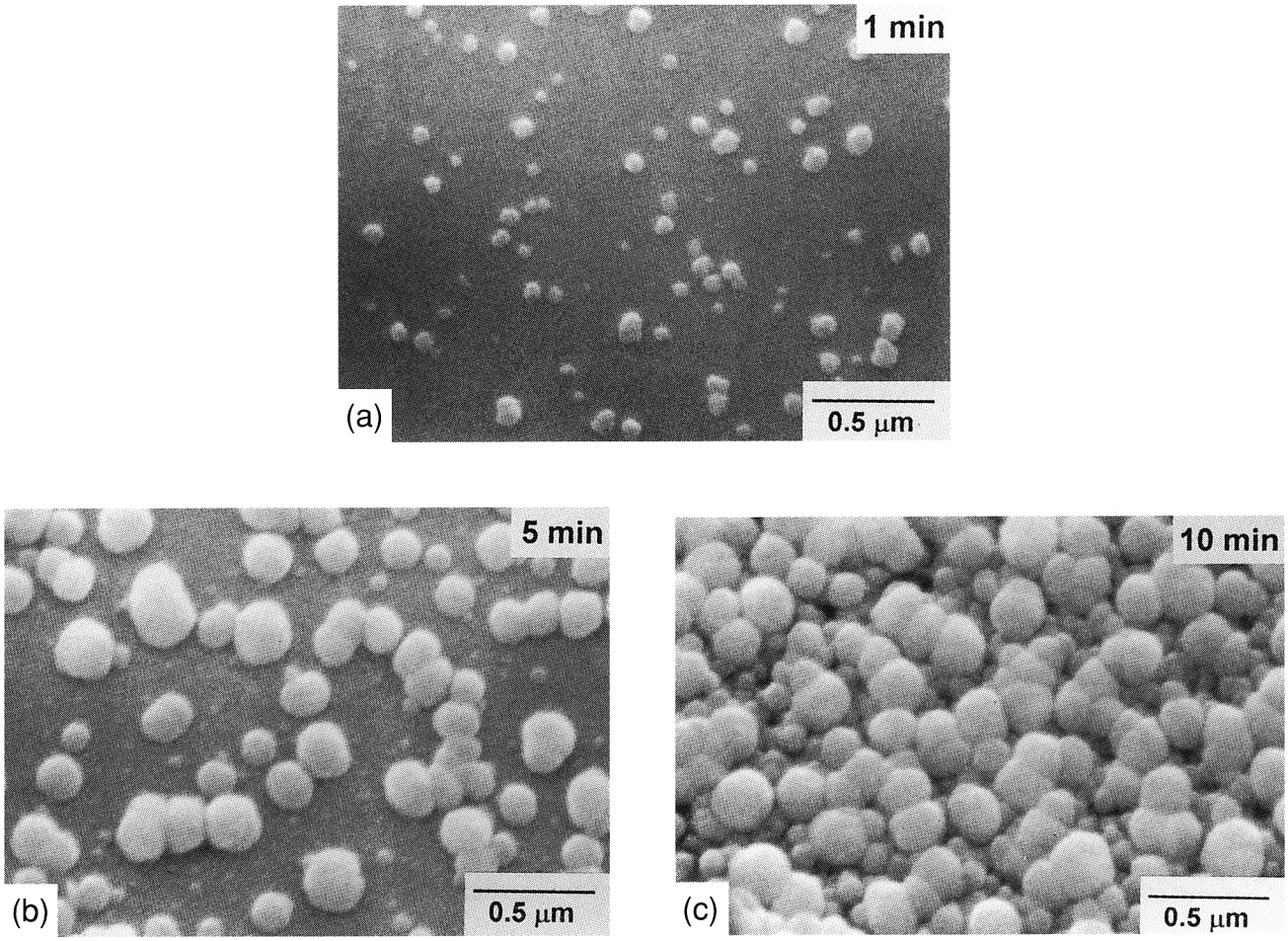

Fig. 10. Growth of a $BaTiO_3$ film in 0.5*M* $Ba(OH)_2$ at 70°C after (A) 1 min, (B) 5 min, (C) 10 min.

$[Ba^{2+}]$ increased the stability of $BaTiO_3$ (analogous to undercooling in solidification), thereby increasing the nucleation rate. Increasing the temperature enhanced the probability that a critical nucleus could surmount the activation barrier to become a stable nucleus for crystal growth. Increasing the temperature may have increased the growth rate of the $BaTiO_3$ particles, but the observation that the grain size decreased with increasing temperature implied that the ratio of nucleation rate to growth rate increased. The observation of particles appearing first on the precursor film surface was consistent with heterogeneous nucleation, which occurred preferentially at free surfaces.

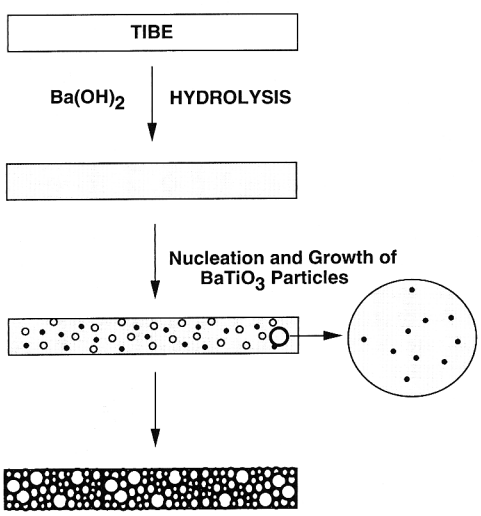

Fig. 11. Schematic illustration of sequence of events of hydrothermal $BaTiO_3$ film formation.

The development of large pores or discontinuities in the large grain films (Figs. 5(a), 7(a), 8(a)) is analogous to experiments on the instability of polycrystalline thin films by Agrawal and Raj,[18] Kennefick and Raj,[19] and Miller *et al.*[20] They observed that when the grain size of a film was larger than the film thickness, the film began to break up, revealing the substrate. In their case, the thin films were initially dense, and film breakup proceeded by diffusional coarsening mechanisms at $0.5T_m$ and above. In our case, film breakup was associated with the nucleation and growth behavior of the film. Consider two extreme cases. When the distance between nucleation sites is large compared to the film thickness, the particles will be isolated from one another, and the film will be discontinuous. If the distance between nucleation sites is small compared to the film thickness, a continuous film will form, with porosity restricted to interstices between grains. Somewhere between these extremes (i.e., as the nucleation spacing approaches the film thickness) the film will begin to develop discontinuities or pores that are larger than interstitial sites between close-packed particles.

V. Summary

We have demonstrated the utility of hydrothermal processing to form $BaTiO_3$ films from organometallic precursors at 80°C and below. The films were cubic, and contained hydroxyl groups as well as impurities containing sodium and silicon. Film formation was facilitated by increasing $[OH^-]$, $[Ba^{2+}]$, and the temperature. The same conditions that facilitated film formation caused the grain size of the films to decrease,

resulting in transparent films of $BaTiO_3$ with a grain size of ≈0.1 μm. The observations indicated that the grain size of the films depended on the nucleation rate of the $BaTiO_3$ particles.

Acknowledgments: We wish to acknowledge helpful discussions with Fatih Dogan and Matt Trau and the assistance of Edward Vicenzi for the microprobe measurements.

References

[1]W. D. Kingery, H. K. Bowen, and D. R. Uhlmann, *Introduction to Ceramics*, 2nd ed; Ch. 18. Wiley, New York, 1976.

[2]C. J. Brinker and G. W. Scherer, *Sol–Gel Science*. Academic Press, London, U.K., 1989.

[3]L. F. Francis, Y.-J. Oh, and D. A. Payne, "Sol–Gel Processing and Properties of Lead Magnesium Niobate Powders and Thin Layers," *J. Mater. Sci.*, **25**, 5007–13 (1990).

[4]R. M. Barrer, *Hydrothermal Chemistry of Zeolites*. Academic Press, London, U.K., 1982.

[5]E. Lilley and R. R. Wusirika, "Method for the Production of Mono-size Powders of Barium Titanate," U.S. Pat. No. 4 764 493, August, 1988.

[6]F. Dogan, J. Liu, M. Sarikaya, and I. A. Aksay, "A Study on the Formation of Hydrothermally Prepared $BaTiO_3$ Particles," *Proc.—Annu. Meet., Electron. Microsc. Soc. Am., 50th*, 304–305 (1992).

[7]M. M. Lencka and R. E. Riman, "Thermodynamic Modeling of Hydrothermal Synthesis of Ceramic Powders," *Chem. Mater.*, **5**, 61–70 (1993).

[8]N. Ishizawa, H. Banno, M. Hayashi, S. E. Yoo, and M. Yoshimura, "Preparation of $BaTiO_3$ and $SrTiO_3$ Polycrystalline Thin Films on Flexible Polymer Film Substrate by Hydrothermal Method," *Jpn. J. Appl. Phys.*, **29** [11] 2467–72 (1990).

[9]P. Bendale, S. Venigalla, J. R. Ambrose, E. D. Verink Jr., and J. H. Adair, "Preparation of Barium Titanate Films at 55°C by an Electrochemical Method," *J. Am. Ceram. Soc.*, **76** [10] 2619–27 (1993).

[10]E. B. Slamovich and I. A. Aksay, "Hydrothermal Processing of $BaTiO_3$/Polymer Films," *Mater. Res. Soc. Symp. Proc.*, **346**, 63–68 (1994).

[11]H. Galsater, *pH Measurement*. VCH, Weinheim, Germany, 1991.

[12]K. Uchino. E. Sadanaga, and T. Hirose, "Dependence of the Crystal Structure on Particle Size in Barium Titanate," *J. Am. Ceram. Soc.*, **72** [8] 1555–58 (1989).

[13]W. Y. Shih, W.-H. Shih, and I. A. Aksay, "Size Dependence of the Ferroelectric Transition of Small $BaTiO_3$ Particles: Effect of Depolarization," *Phys. Rev. B*, **50** [21] 15, 575–85 (1994).

[14]C. Sanchez, F. Babonneau, S. Doeuff, and A. Leaustic, "Chemical Modifications of Titanium Alkoxide Precursors"; in *Ultrastructure Processing of Advanced Ceramics*. Edited by J. D. Mackenzie and D. R. Ulrich. Wiley, New York, 1988.

[15]K. Nakamoto, *Infrared and Raman Spectra of Inorganic and Coordination Compounds*, 4th ed. Wiley, New York, 1986.

[16]D. Hennings and S. Schreinmacher, "Characterization of Hydrothermal $BaTiO_3$," *J. Eur. Ceram. Soc.*, **9**, 41–46 (1992).

[17]P. K. Dutta and J. R. Gregg, "Hydrothermal Synthesis of Tetragonal Barium Titanate," *Chem. Mater.*, **4**, 843–46 (1992).

[18]D. C. Agrawal and R. Raj, "Autonucleation of Cavities in Thin Ceramic Films," *Acta Metall.*, **37** [7] 2035–38 (1989).

[19]C. M. Kennefick and R. Raj, "Copper on Sapphire: Stability of Thin Films at 0.7 T_m," *Acta Metall.*, **37** [11] 2974–52 (1989).

[20]K. T. Miller, F. F. Lange, and D. B. Marshall, "The Instability of Polycrystalline Thin Films: Experiment and Theory," *J. Mater. Res.*, **5** [1] 151–60 (1990).

[21]C. M. Chun, F. Dogan, and I. A. Aksay, unpublished results.

[22]W. Hertl, "Kinetics of Barium Titanate Synthesis," *J. Am. Ceram. Soc.*, **71** [10] 879–83 (1988).

[23]D. A. Porter and K. E. Easterling, *Phase Transformations in Metals and Alloys*. Van Nostrand Reinhold, U.K., 1981).

[24]M. Avrami, "Kinetics of Phase Change, I: General Theory," *J. Chem. Phys.*, **7**, 1103–12 (1939). □